SENSORS

Sustainable manufacturing of sensors onto soft systems using self-coagulating conductive Pickering emulsions

Sang Yup Kim[1], Youngwoo Choo[2], R. Adam Bilodeau[1,3], Michelle C. Yuen[1]*, Gilad Kaufman[2], Dylan S. Shah[1], Chinedum O. Osuji[2†], Rebecca Kramer-Bottiglio[1‡]

Compliant sensors based on composite materials are necessary components for geometrically complex systems such as wearable devices or soft robots. Composite materials consisting of polymer matrices and conductive fillers have facilitated the manufacture of compliant sensors due to their potential to be scaled in printing processes. Printing composite materials generally entails the use of solvents, such as toluene or cyclohexane, to dissolve the polymer resin and thin down the material to a printable viscosity. However, such solvents cause swelling and decomposition of most polymer substrates, limiting the utility of the composite materials. Moreover, many such conventional solvents are toxic or otherwise present health hazards. Here, sustainable manufacturing of sensors is reported, which uses an ethanol-based Pickering emulsion that spontaneously coagulates and forms a conductive composite. The Pickering emulsion consists of emulsified polymer precursors stabilized by conductive nanoparticles in an ethanol carrier. Upon evaporation of the ethanol, the precursors are released, which then coalesce amid nanoparticle networks and spontaneously polymerize in contact with the atmospheric moisture. We printed the self-coagulating conductive Pickering emulsion onto a variety of soft polymeric systems, including all-soft actuators and conventional textiles, to sensitize these systems. The resulting compliant sensors exhibit high strain sensitivity with negligible hysteresis, making them suitable for wearable and robotic applications.

INTRODUCTION

Compliant sensors are becoming important components in the fields of biomedicine (*1*–*3*), sports (*4*, *5*), and robotics (*6*–*8*) as a way to communicate between the user and device by eliciting reliable state information, such as body movements or deformations. Compliant and geometrically complex soft robotic systems require integrated sensors that can stretch and conform along surface contours while adding negligible stiffness to the system (*9*–*12*). Over the last decade, conductive composite materials have gained traction as wearable, stretchable sensors because of their scalability in manufacturing processes (*13*–*20*), an attribute that is difficult to achieve using other strategies such as patterned conductive traces (*21*–*24*) or fluidic channels filled with conductive liquid (*25*–*28*). Conductive composite-based sensors consist of polymer matrices and conductive fillers, and these sensors can be designed to measure deformation via changes in electrical resistance or capacitance. These devices are typically fabricated by a liquid molding process that comprises a distribution of solid-phase fillers into liquid-phase resins and subsequent casting of the filler/resin mixture. Hence, obtaining sufficient resin flow during this process is critical for quality control, leading to widespread use of solvents (e.g., toluene, cyclohexane, and hexane) to dissolve the polymer resin and thin down the material (*29*–*31*).

However, critical issues arise because of the typically high concentration of such solvents in the resin/filler mixture [ca. >70 volume % (vol %)], such as prolonged postprocesses to evaporate the solvents (*32*) and a dangerous manufacturing environment (*33*). Moreover, solvents capable of dissolving polymer resins can also penetrate into cross-linked polymer networks and cause undesirable swelling and degradation of the host structure (*34*), be it a robot or a human. For example, printing a cyclohexane-containing resin/filler mixture onto an inflated latex balloon results in the immediate bursting of the balloon. The use of nonconventional solvents, such as ethanol (EtOH) and water, in lieu of conventional solvents, has thus far been infeasible because they poorly dissolve most polymer resins, leading to the creation of an emulsion with two distinct phases when mixed instead of the desired homogeneous solution.

Here, we addressed these challenges using an EtOH-based Pickering emulsion stabilized by nanoparticles (*35*–*37*). Using EtOH, instead of conventional solvents, enabled a multitude of wearable and robotic systems, including self-sensing McKibben actuators and hybrid robotic textiles, to be realized through a sustainable manufacturing process. Our Pickering emulsion allowed us to print directly onto the bare polymer surfaces of all-soft actuators for monitoring surface strains. Pickering emulsions were also printed onto conventional polymer textiles to fabricate wearable sensors that measure strain values with high sensitivity and negligible hysteresis.

RESULTS

Characteristics of self-coagulating conductive Pickering emulsions

Our study was inspired by hemostasis, a natural bodily process achieved by blood plasma that delivers proteins and platelets to an open wound (*38*). The wound healing process is rapid and efficient

[1]Mechanical Engineering and Material Science, School of Engineering and Applied Science, Yale University, 9 Hillhouse Ave., New Haven, CT 06511, USA. [2]Chemical and Environmental Engineering, School of Engineering and Applied Science, Yale University, 9 Hillhouse Ave., New Haven, CT 06511, USA. [3]School of Mechanical Engineering, Purdue University, 585 Purdue Mall, West Lafayette, IN 47907, USA.
*Present address: Materials and Manufacturing Directorate, Air Force Research Laboratory, Wright-Patterson Air Force Base, OH 45433, USA.
†Present address: Department of Chemical and Biomolecular Engineering, University of Pennsylvania, 220 S 33rd St., Philadelphia, PA 19104, USA.
‡Corresponding author. Email: rebecca.kramer@yale.edu

because of the direct transportation of microscale substances and their spontaneous coagulation (*39*). We adopted the fundamentals of hemostasis to composite materials and their manufacturing to fabricate composite-based sensors in a sustainable fashion. We used a Pickering emulsion that consists of carbon black (CB) as stabilizing nanoparticles, polydimethylsiloxane (PDMS) precursors as the dispersed phase, and EtOH as the continuous phase and directly print it onto polymer substrates (e.g., sheet or textile) to infuse conductive composite materials (Fig. 1). We call this emulsion a self-coagulating conductive Pickering (SCP) emulsion. Upon printing of the SCP emulsion and evaporation of EtOH, the colloids relaxed onto the substrate, and the low viscosity of the PDMS precursors promoted the release and fusion of precursors amid the CB conductive network. One-part PDMS precursors were then rapidly polymerized in contact with atmospheric moisture without additional processing steps involving heat or pressure. As a result, a polymer substrate spontaneously acquired an infused conductive composite while avoiding issues with swelling or degradation of the substrate.

We began by analyzing the morphology and rheological behavior of SCP emulsions (Fig. 2). An SCP emulsion was prepared in under 10 min by sonicating as-received CB in an EtOH medium for 6 min, adding PDMS precursors to the CB/EtOH suspension, and subsequently sonicating for 2 min. Optical micrographs of the emulsion show CB/PDMS-precursor droplets in the size range of a few micrometers while present in the EtOH medium (Fig. 2A). Scanning electronic microscope (SEM) imaging performed on the CB/PDMS droplets cured within the medium confirmed that the CB/PDMS-precursor droplets are spherical in shape and covered with CB nanoparticles (Fig. 2B). Freeze-fractured specimens further revealed the core-shell structure, where the CB shell encapsulates the PDMS-precursor core.

Dynamic light scattering measurements of SCP emulsions showed the coexistence of residual CB nanoparticles and CB/PDMS-precursor droplets in the emulsion and that the droplet size tends to decrease with increasing CB content (Fig. 2C). The average diameter (<2.0 μm) of CB/PDMS-precursor droplets was expected to facilitate a uniform CB distribution in the PDMS matrix by suppressing the formation of resin-rich regions greater than the droplets' sizes. We have not observed milli/microscale agglomerations of CB nanoparticles in the resulting composite, even at >20 weight % (wt %) of CB concentrations. Ultraviolet-visible (UV-vis) transmittance measurements performed on the diluted SCP emulsion revealed the stability of the emulsion against sedimentation or creaming, using absorbance retention as an indication of the settling of substances (Fig. 2D). We achieved a stable emulsion at CB concentration >10 wt % with respect to PDMS precursor alone, retaining >95% of the absorbance, which is in contrast to the unstable emulsion after 2 weeks (see inset of Fig. 2D). The higher stability obtained at higher concentrations of electrically conductive CB also facilitated the creation of electrical pathways in the final composite material, which is essential for sensing applications.

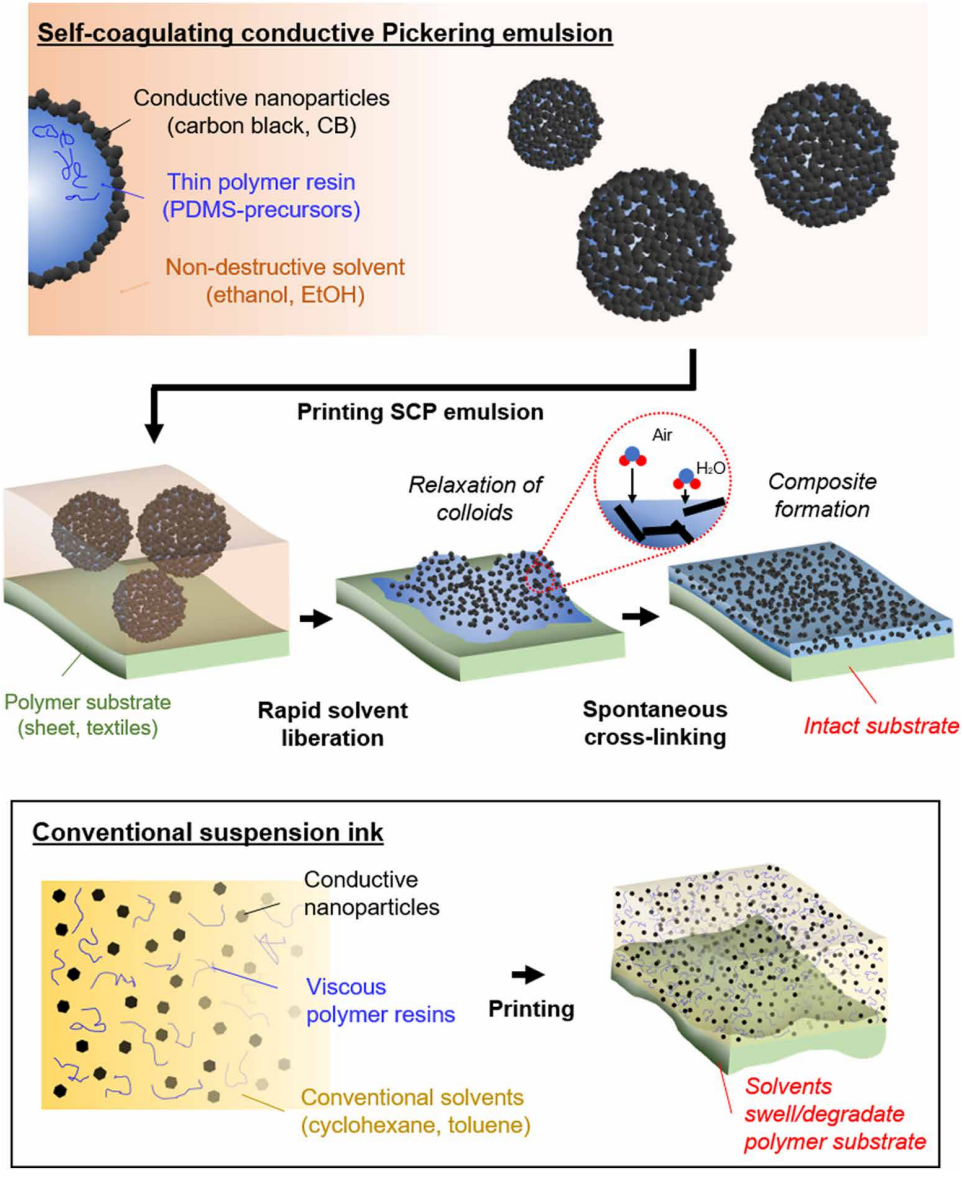

Fig. 1. Illustration of SCP emulsion and the printing process. SCP emulsion consists of PDMS precursors stabilized by CB nanoparticles in an EtOH medium. Printing SCP emulsion onto polymer substrates initiates a cascade reaction that spontaneously forms the conductive composite. Using EtOH as the medium enables a sustainable printing process without swelling or degradation of the polymer substrate, a typical drawback when using conventional suspension inks with harsh, often toxic solvents. The nondestructive characteristic of SCP emulsions unlocks opportunities to integrate complaint sensors into soft systems.

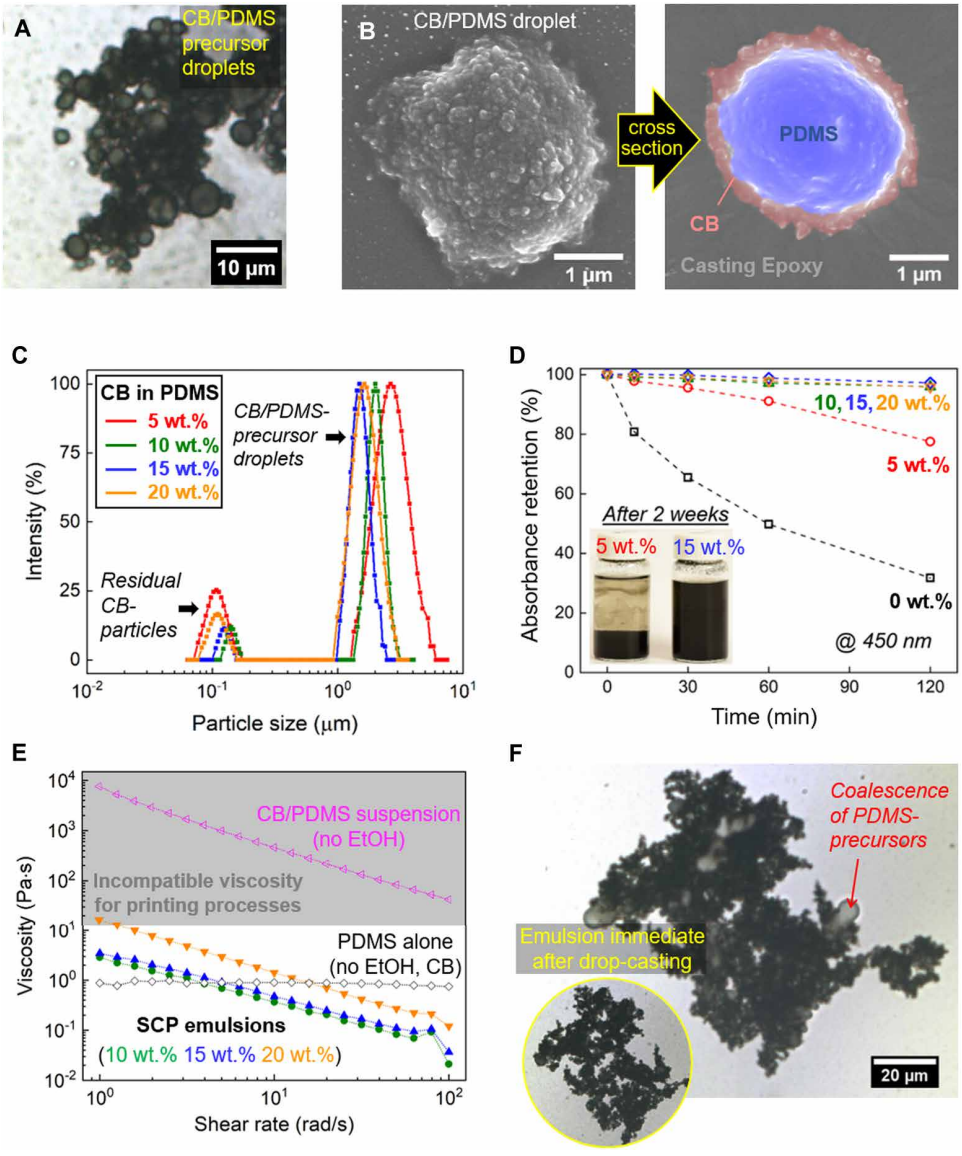

Fig. 2. Material characteristics and rheological behavior of SCP emulsions. (**A**) Optical micrograph of CB/PDMS-precursor droplets within EtOH medium. (**B**) SEM images of a CB/PDMS droplet cured within EtOH medium and its freeze-fractured morphology. The cross-sectional image is false-colored to highlight the PDMS core (blue) and the CB shell (red). (**C**) Dynamic light scattering results for the size distribution of the emulsion at various CB concentrations. The average diameter for the droplets is around 2 μm. (**D**) Absorbance retention of the emulsions with varying CB concentrations, obtained from UV-vis measurements at 450 nm. The inset image shows SCP emulsions at 5 and 15 wt % after 2 weeks. (**E**) The rheological profile of a PDMS precursor alone, a CB/PDMS suspension, and SCP emulsions. EtOH thins out a CB/PDMS suspension to a printable viscosity, and the colloids in SCP emulsions exhibit a shear-thinning behavior. (**F**) Release and coalescence of PDMS precursors when printed onto a glass slide and EtOH evaporates. Coalesced PDMS precursors spontaneously polymerize in contact with atmospheric moisture.

SCP emulsions exhibited shear-thinning behavior, which is beneficial for the nozzle-assisted printing process, and the EtOH content determined the overall viscosity (Fig. 2E and fig. S1). For example, the SCP emulsion containing 95 vol % of EtOH exhibited a 1000-fold lower viscosity compared to the CB/PDMS mixture alone. Such low viscosity allowed CB/PDMS-precursor droplets to create a uniform composite layer and permeate through various types of textile substrates. Upon printing, the EtOH medium rapidly evaporated, CB/PDMS-precursor droplets relaxed onto the substrate, and PDMS precursors were released from the CB shell, fusing together to form a monolithic composite (Fig. 2F). The entire process was rapidly accomplished upon evaporation of the EtOH. We surmise that the coalescence of CB/PDMS-precursor droplets can be further controlled by tuning the substrate material and texture (*40*). The resulting infused droplets rapidly cured at ambient conditions in contact with the atmospheric moisture because the precursor contains hydroxy-terminated PDMS and a cross-linker [tris(cyclohexylamino)methylsilane], which triggers a two-step curing reaction when exposed to the moisture. As a result, relaxed CB/PDMS-precursor droplets spontaneously became a conductive composite material.

SCP emulsion printed onto bare polymer substrate

We created conductive composites on the bare surface of the cured Ecoflex 00-30 substrates by directly printing SCP emulsion and characterized the electromechanical properties of the resulting composites (Fig. 3). The sheet resistance of the produced composite was dependent on the CB concentration in the PDMS matrix and the composite morphology (Fig. 3A). Higher CB content, with respect to PDMS precursors, generally increased the local electrical conductivity and also stimulated the formation of wrinkles and microscale cracks on the composite (see inset images of Fig. 3A). An SEM image of a conductive composite at 15 wt % of CB concentration shows the wrinkled surface morphology, and a transmission electron microscopy (TEM) image further reveals the presence of embedded CB nanoparticles (Fig. 3B). Such wrinkles further developed into microscale cracks at >15 wt % CB content, presumably attributed to the clustering of colloids as EtOH evaporates (*41*), and the resulting composite morphology enabled low-hysteresis, high-sensitivity strain sensing. However, at >25 wt % CB content, the composite was easily delaminated from the substrate, thus degrading its value as a sensor.

The microstructure of conductive composites, consisting of wrinkles and microcracks, allowed the composite to stretch without introducing damage by leveraging the opening of existing cracks (Fig. 3C). For example, in the case of printing a control ink containing cyclohexane, a composite film devoid of wrinkles/cracks catastrophically failed at the strain of 180% because the composite material itself was insufficiently stretchable. However, when SCP emulsion at 20 wt % was printed, the composite film could accommodate applied

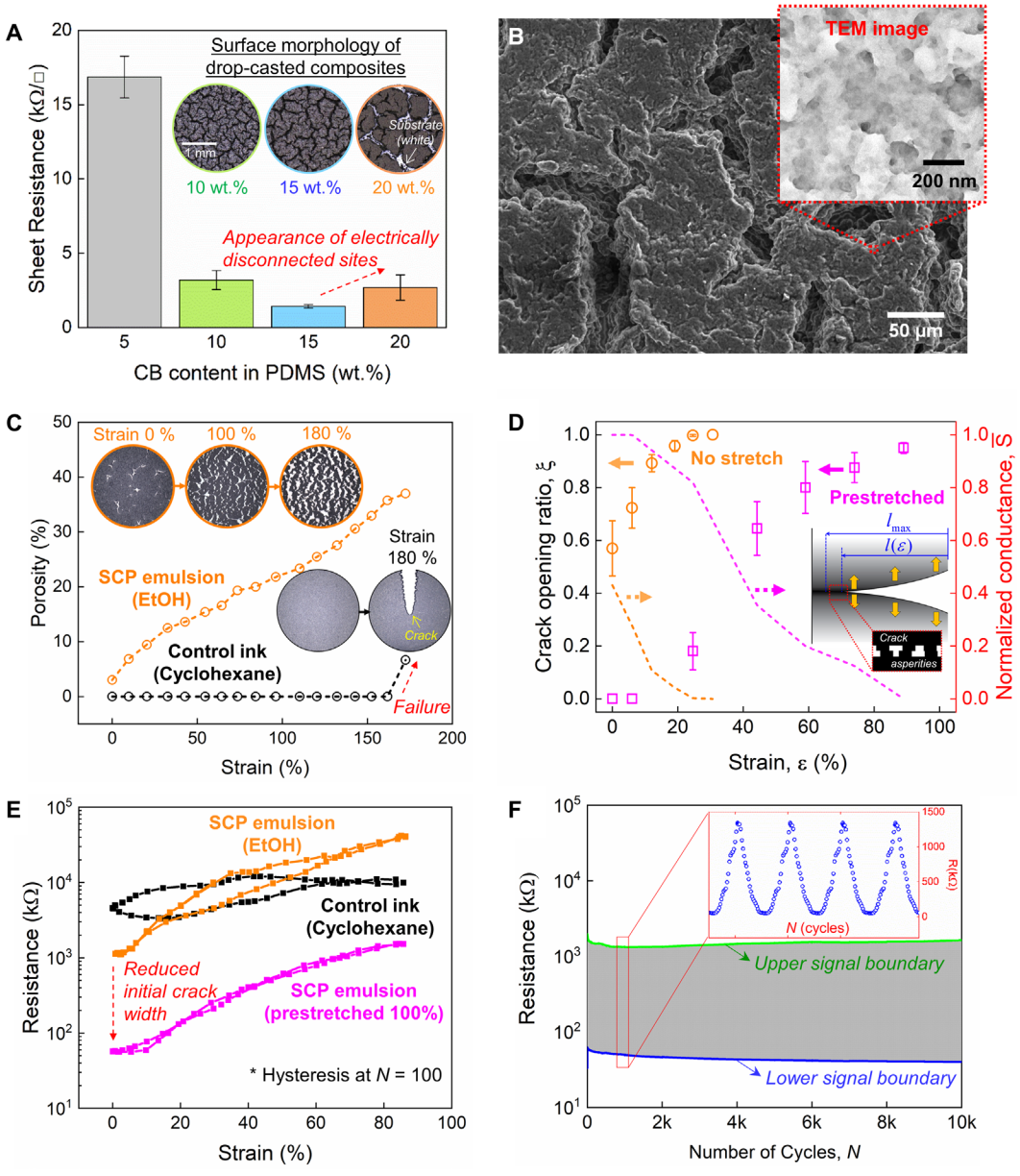

Fig. 3. Characteristics of conductive composites directly printed onto bare polymer substrates. (**A**) Sheet resistance of the composites and their surface morphology. Wrinkles/cracks formed as EtOH evaporates become apparent with an increasing CB concentration. (**B**) SEM image of the composite surface at a 15 wt % CB concentration and TEM inset image revealing uniformly distributed CB nanoparticles. (**C**) Porosity of composites as a function of applied strains. Composite microstructure consisting of microscale cracks give rise to the stretchability (SCP emulsion), different from the crack-free composites that exhibit a catastrophic failure (control ink). (**D**) Measured crack opening ratio in composites and the normalized electrical conductance predicted from the measured data and the inset crack opening model. Error bars indicate 1 SD. Printing SCP emulsions onto a prestretched substrate (at ε = 100%) decreases the initial crack width (at ε = 0%), thereby increasing the working strain range from ca. 20 to 100%. (**E**) Hysteresis in mechanoelectrical responses of the composites produced on Ecoflex 00-30 substrates. Crack opening mechanism of the SCP emulsion sensor grants negligible hysteresis and high sensitivity to strain within the working strain range. (**F**) Long-term fatigue behavior of the composite sensor produced from SCP emulsions.

strain by opening up its existing cracks, as evidenced from the increased porosity shown in Fig. 3C. Furthermore, the crack opening mechanism gave rise to the sharp increase in the electrical resistance with increasing strain because the separation of crack planes induces a sudden disconnection (see fig. S2 for details). We call this underlying principle a crack opening sensing mechanism, which is a modification of the crack-driven model in (*23*). When the crack opening ratio is defined as $\xi(\varepsilon)$, our sensing mechanism predicts the normalized electrical conductance across a crack ($\overline{S}$) as $\overline{S} = 1 - \xi$ (see Materials and Methods for details).

This simple underlying principle provides a route to tailor the range of working strains by leveraging the width of existing cracks, as shown in Fig. 3D. Compared to printing SCP emulsions onto a pristine substrate, stretching the substrate before the printing decreased

the initial crack separation (from $\xi_0 = 0.6$ to 0.0), thereby increasing the range of working strains (from 20 to 80%). The electromechanical response of the composite sensors manifests the crack opening sensing mechanism (Fig. 3E). A composite sensor produced from a control ink exhibits high hysteresis and low stain sensitivity because its electrical resistance is solely determined by the shape change of the composite. On the other hand, composite sensors printed from SCP emulsions reveal negligible hysteresis and high sensitivity to strains, driven by the crack opening sensing mechanism. Furthermore, the appearance of hysteresis at $\varepsilon > 20\%$ for the composite produced on a pristine substrate is in agreement with the prediction in Fig. 3D (working strain of 20%), and the further increase in the resistance is expected to be from the geometrical shape change, not the crack opening.

Cyclic tests performed on the composite fabricated onto a prestretched substrate reveal consistent sensor responses when the composite is stretched up to 100% (Fig. 3F). We expect that such reliable response is due to the wrinkled/cracked composite structure that redistributes applied strains and minimizes the strain concentration. In sum, printing SCP emulsions onto bare polymer substrates demonstrates a facile, rapid, and safe process to implement quality sensors (i.e., negligible hysteresis and high strain sensitivity) directly onto soft systems.

SCP emulsions printed into textile substrates

To broaden the use of our sensors, we printed SCP emulsions into textiles to embed sensing capabilities into wearables (Fig. 4). Upon direct printing of SCP emulsions onto a textile, CB/PDMS-precursor droplets permeated through the textile and formed a conductive composite conformally around the textile fiber rovings (Fig. 4A). Optical micrographs of a polyester/spandex textile onto which SCP emulsion was printed reveal CB/PDMS composites infused into the textile (Fig. 4B). The infused composites maintained the fiber architecture of the textile, rather than creating a thick composite layer on top, thereby preserving porosity that grants breathability and comfort for wearable applications (fig. S3). In addition, printing SCP emulsions into textiles propelled evaporation of the solvent as the EtOH medium separated from CB/PDMS-precursor droplets and rapidly absorbed into the textile (fig. S4). This separation of active materials (CB/PDMS precursor) from a vehicle (EtOH) grants an effective printing process that locally infuses a sufficient amount of conductive material, even after just a single printing pass.

SEM imaging further confirms that individual fiber rovings of the textile were coated with the infused composites (Fig. 4C). The infused composites exhibit microcracks on the top surface where CB/PDMS-precursor droplets have penetrated through the textile because of the ample fiber-interstitial spaces (ca. >10 μm) that are greater than the precursor droplet size (*42*). Such generic microcracks further assisted in preserving inherent textile properties and rendered a strain-sensing ability that exploits aforementioned crack opening behavior (*23*). The permeating CB/PDMS-precursor droplets allowed the final composites to infuse deep into the textile and obtain an interpenetrating structure with textile fibers for a secure bond (fig. S5). TEM imaging reveals that CB nanoparticles were well distributed along a PDMS matrix of 200-nm thickness to grant consistent electrical properties, even when the composite layer was thinner than the precursor droplet diameter (Fig. 4D).

Consequently, printing SCP emulsions created quality conductive composite-infused textiles that can be used as resistive strain sensors. Notably, polyester/spandex textile sensors exhibited a similar tensile modulus to the neat textiles (Fig. 4E). The increment of the tensile modulus induced by the SCP emulsion was <30%, which is significantly lower than the >200% for textiles onto which the control suspension was printed (fig. S6). Such minimal mechanical footprint of the infused composite is advantageous for wearable applications, which necessitate conformability and stretchability. The sheet resistance of the textile sensors was higher than that of the infused composites alone because the textile fibers are not electrically conductive. Such resistance of the textile reached the minimum value around 15 wt % of CB concentration, presumably because of the generic crack formation, a behavior also observed from the composites printed onto bare polymer substrates (see Fig. 3A).

Stretching composite-infused polyester/spandex textiles increased their electrical resistance with negligible hysteresis after the initial ~10 cycles of Mullins softening (*43*), and CB concentrations in the PDMS matrix modulated such electrical responses (Fig. 4F). For example, a composite-infused textile at 10 wt % CB concentration elicited an 810% increase in the resistance when stretched, which is significantly higher than 260% for a textile at 15 wt % CB concentration. Likewise, similar to the composite-printed bare polymer substrates, these textile sensors exhibited high sensitivity to strains (i.e., gauge factor >30) and negligible hysteresis. Uniaxial fatigue testing performed at 17% strain reveals the consistent electrical response of a textile sensor over 10,000 cycles, demonstrating the mechanical robustness of the infused composite (Fig. 4G). Such fatigue resistance was achieved through precise control of CB concentrations and printing directions (fig. S7).

We also printed the SCP emulsion onto various textile substrates (i.e., kinesiology tape and cotton) and investigated their electrical characteristics (Fig. 4H). Both the strain sensitivity and the working strain (linear response) of the textile sensors are governed by the substrate textile's fiber architecture. For example, the working strains are 4.6, 12, and 28% for textile sensors using kinesiology tape, spandex, and cotton, respectively. Increasing the fiber packing density in a textile results in higher working strain and an inversely lower strain sensitivity. Such tunability of sensor characteristics using substrate textiles further supports that the sensing mechanism is associated with crack asperities rather than the composite's geometrical shape change. As a result, the strain sensitivity reached a gauge factor of up to 150 when SCP emulsion was printed onto kinesiology tape with coarsely packed fibers, enabling its use as an ultrasensitive strain sensor.

Sensor integration onto all-soft systems through directly printed sensors

When printed onto bare polymer surfaces, SCP emulsions enabled direct strain monitoring of various types of all-soft systems widespread in soft robotics (Fig. 5). SCP emulsions were printed onto the all-soft systems to directly create strain sensors and maintain the original pressure-responsive behaviors. SCP emulsion consisting of EtOH broadened the selection of compatible substrates for printing by mitigating the damage caused from the contained solvent. Our presented method is thus capable of printing composite sensors onto a pressurized balloon, which has been impossible to achieve because of the catastrophic failure of balloons when exposed to conventional solvents (movie S1).

When SCP emulsions were printed onto a pressurized latex balloon, the printed sensor could be used to monitor the inflation of the

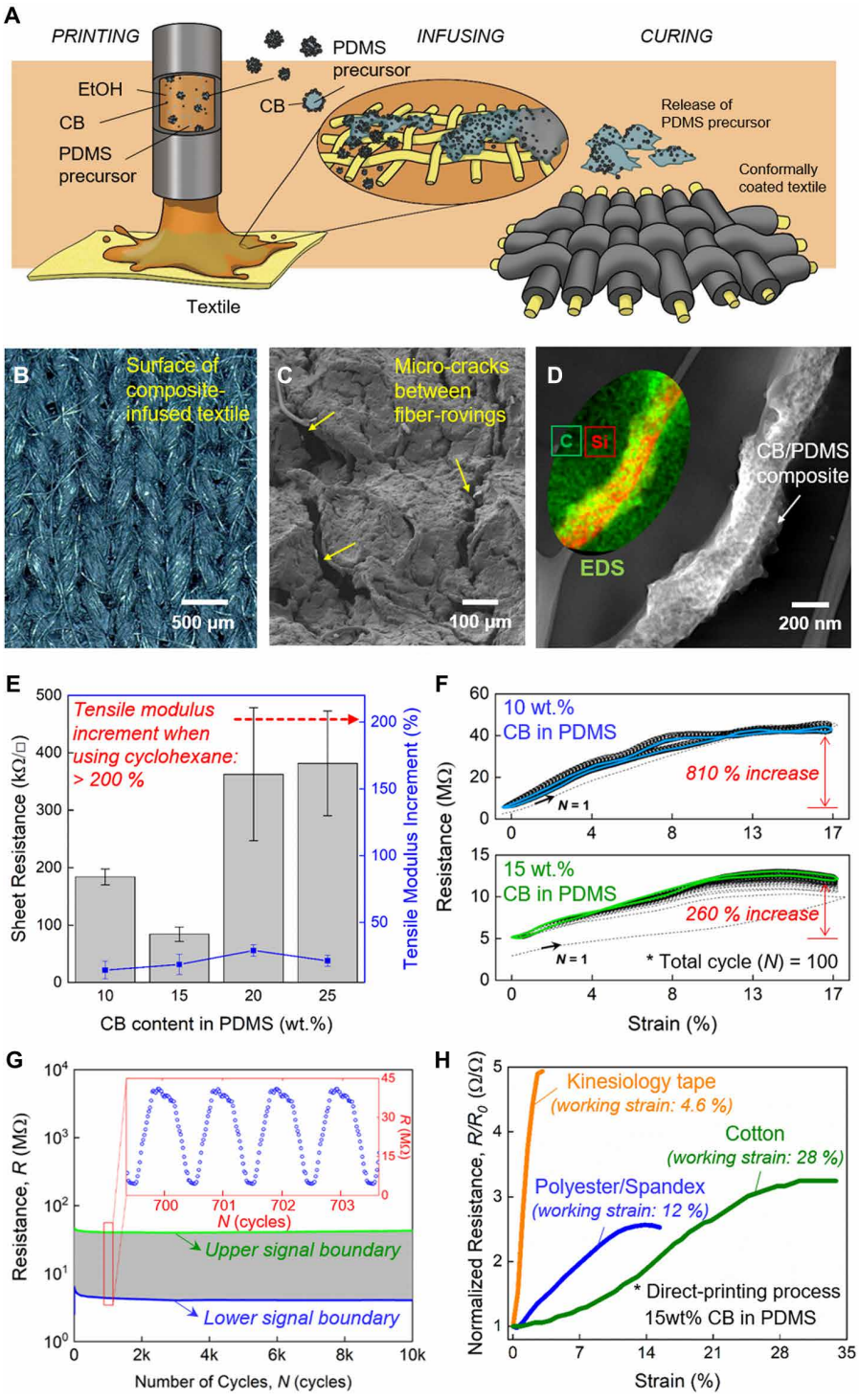

Fig. 4. Morphology of CB/PDMS composites infused into textiles. (**A**) Illustration of the direct printing of SCP emulsions into textiles. (**B**) Optical micrograph of the surface of a composite-infused textile. (**C**) SEM image of the infused composite that contains generic microcracks on the surface. (**D**) TEM images of a thin CB/PDMS composite layer bonded to the textile fiber. EDS result confirms the wet-out of the textile with the PDMS matrix. (**E**) Sheet resistance of composite-infused textiles and the tensile modulus increment due to the composite. Error bars indicate 1 SD. Composites from SCP emulsions add negligible stiffness to the textile, unlike that from a control ink. (**F**) Electrical resistance of composite-infused polyester/spandex textiles during uniaxial cyclic loading for the initial 100 cycles (*N*). Highlighted curves indicate $N = 50$. (**G**) Long-term fatigue behavior of the composite-infused polyester/spandex textile. The inset shows a detailed electrical resistance as a response to a sinusoidal uniaxial displacement. (**H**) Strain-responsive electrical resistances of composite-infused textiles with various substrate textiles.

balloon (Fig. 5A and movie S2). The printed sensor negligibly affected the inflation trajectory of the balloon, and its electrical resistance increased as the balloon inflated. Such a resistance-inflation relation enabled the estimation of the state of inflation of the latex balloon with ca. 9.8% error (see fig. S8). In addition, because the sensors do not perturb the original inflation trajectory of the balloon, SCP emulsions can be printed at different angles with respect to the balloon's width (i.e., 0°, 45°, and 90°) and used to elucidate the directionality of the balloon's inflation/deflation (Fig. 5B).

We also printed SCP emulsions onto typical soft robotic actuators, composed of Ecoflex 00-30 silicone elastomer, to monitor the movements of the actuators. For example, by implementing the composite sensors on an elastomeric gripper (*44*), we monitored the movement of its fingers (Fig. 5C). Similarly, when SCP emulsions were printed onto a fiber-reinforced actuator, the reconfigured motion of the actuator was tracked as the location of a strain-limiting layer was adjusted (Fig. 5D and movie S3). The attached strain-limiting layer was easily detached and reattached using a self-adhesive layer (*45*), thereby applying different bending strains to the sensor. These demonstrations serve to collectively showcase the viability of SCP emulsion in producing sensors for all-soft systems.

To further demonstrate the capability of our composite sensors in prototypical soft systems, we devised self-sensing McKibben actuators, the simplest of which are latex balloon actuators surrounded by a mesh sleeve that brings about either extension or contraction when pressurized (Fig. 6). To date, despite the ubiquity of McKibben actuators in the field of soft robotics, precisely monitoring their actuation has been difficult to achieve. This challenge is attributed to the requisite compliant nature of McKibben actuators, as their intended trajectories can be easily compromised when sensors are separately attached. Our self-sensing McKibben actuators address this issue by seamlessly integrating sensing capabilities into the actuators using a balloon with an SCP-printed trace (Fig. 6A). With the sensor embedded inside of a contraction sleeve, the sensor response tightly corresponds to the

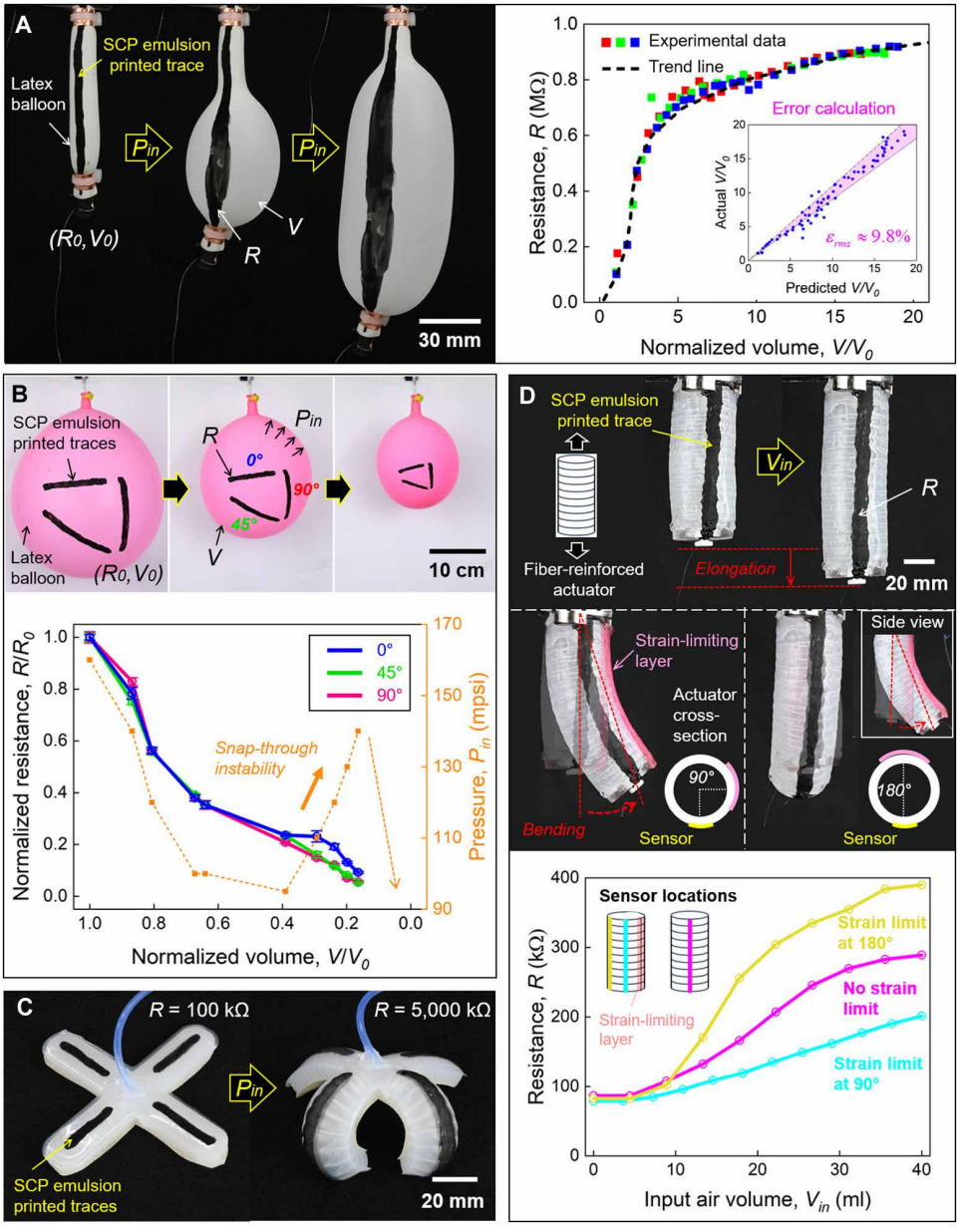

Fig. 5. All-soft systems with directly integrated strain sensors. (**A**) A latex balloon with an integrated composite sensor. Volumetric expansion of the balloon is monitored at <10% of error from the sensor response. (**B**) A spherical latex balloon with SCP emulsion traces printed at varied printing directions (i.e., 0°, 45°, and 90°) to examine any directionality in the volumetric change. Error bars indicate 1 SD. (**C**) A silicone rubber four-legged gripper, onto which SCP emulsion traces are printed. The resistance (*R*) of the trace increases as the gripper inflates. (**D**) A fiber-reinforced silicone rubber actuator with a printed SCP emulsion trace to monitor the strain along the length. A strain-limiting layer is adhered onto the actuator at different locations (i.e., 90° and 180° with respect to the sensor) to create various bending strains.

actuation. Therefore, no additional sensors are necessary to measure the strain of the actuators.

The sensor response of the self-sensing McKibben actuators begins only after the bladder has been inflated to connect with the external mesh, as any sensor information before this only describes the inflation of the inner balloon and not the contraction of the actuator. Any additional inflation of the bladder decreases the resistance in a linear, predictable manner, which allows us to develop a direct correlation between sensor response and the length of the actuator (Fig. 6, B and C). Such electromechanical responses of the sensor, different from a freely expanding balloon, are because the external strain-limiting mesh constrains the expansion of the bladder. The actuation-responsive change in the resistance is apparent and repeatable, allowing for self-sensing closed-loop control of the linear actuators (Fig. 6D and movie S4). We anticipate our self-sensing McKibben actuators to open a new avenue in numerous domains of robotics because they not only minimize the footprint of robotic components but also are easy to manufacture.

Wearable textile sensors

To demonstrate the viability of SCP emulsions, we used textile sensors to monitor strains of arbitrarily shaped, complex systems (Fig. 7). When SCP emulsions were printed into kinesiology tape, the produced textile sensor easily adhered to the convex surface of a fabric-based pneumatic gripper finger using a self-adhesive layer (Fig. 7A). The self-adhesive layer provided close contact between the textile sensor and the gripper finger, which yielded accurate strain measurements and prevented the sensor from delaminating from convex contours (fig. S9). We also show that textile sensors could easily be printed into active clothes that reveal specific motion artifacts present in normal activity (Fig. 7B and movie S5). For example, a kneepad fabricated using a polyester/spandex textile enabled differentiation of gait while walking, climbing, and descending. Ready-made garments (i.e., kinesiology tapes and cotton gloves) were also transformed into smart garments with strain-sensing ability when SCP emulsion was directly printed on (fig. S10).

We further showcased the potential of SCP emulsions by devising a robotic textile, referred to as an OmniSkin, that can be wrapped around inert objects to create robotic systems on demand (Fig. 7C). Our OmniSkin is a hybrid of sensors integrated onto bare polymer substrates (self-sensing McKibben actuator) and textiles (textile sensor) and eliminates the need for attaching separate sensors to monitor strains. In this way, the design and manufacturing processes were significantly simplified compared to the original version of the OmniSkin (*46*), enabling seamless monitoring of multidirectional strains. For example, when applied to a passive foam to elicit inchworm locomotion, our OmniSkin could monitor strains along the length (ε_x) and circumference (ε_y) of the foam, respectively (movie S6). Likewise,

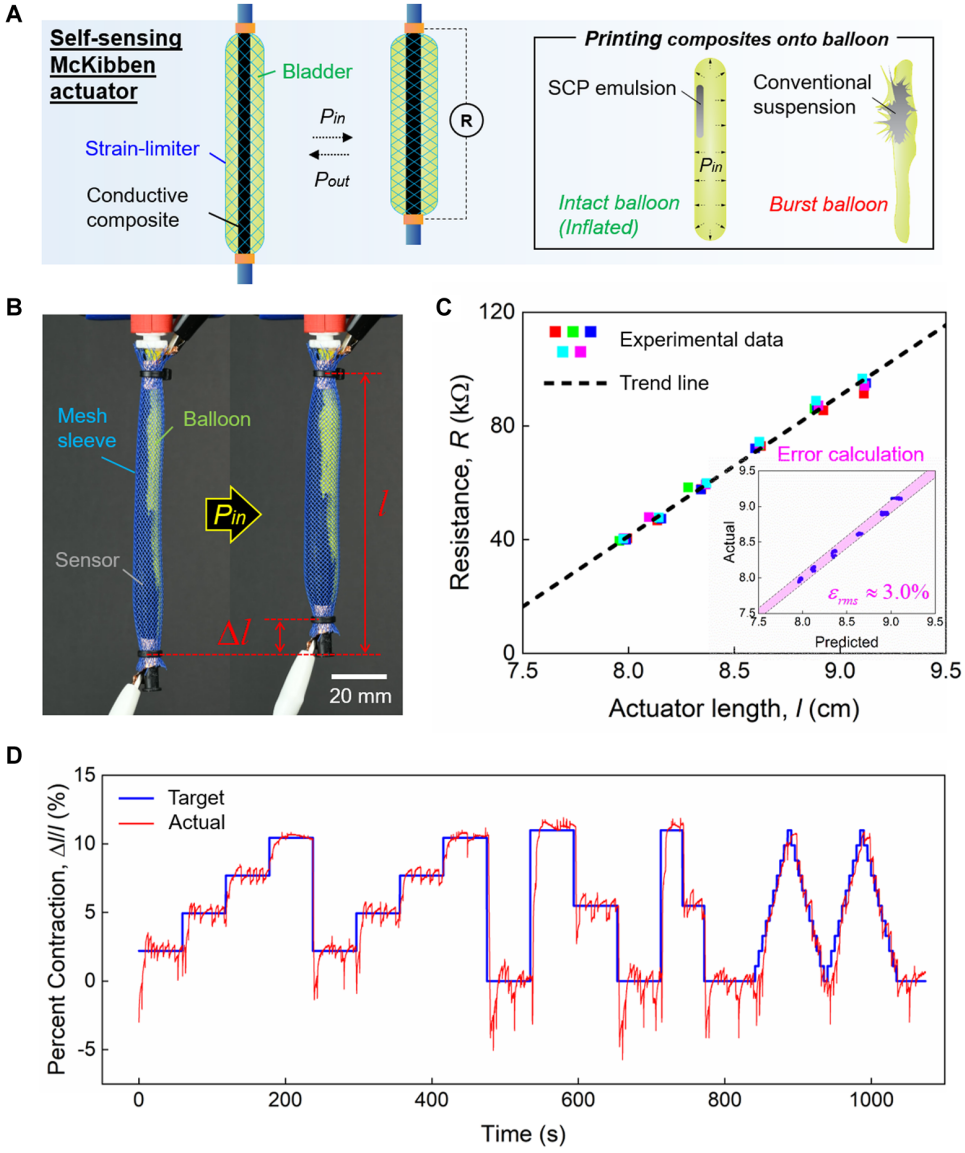

Fig. 6. Self-sensing McKibben actuator. (**A**) Schematic of the self-sensing McKibben actuator, enabled by printing SCP emulsion onto an inflated balloon. P_{in} and P_{out} indicate input pressure and output pressure, respectively, and R denotes the electrical resistance of the sensor. (**B**) Photographs of the actuator that elicits the contraction as the internal balloon inflates. With the input pressure (P_{in}), the initial length (l) of the actuator is decrease by Δl. (**C**) Sensor responses collected from the actuator at various contraction states and the calculated error on the state estimation (predicted length calculated from state estimation compared to ground truth length). The error is quantified as ε_{rms}, a root mean square of the error. (**D**) Closed-looped control of the self-sensing McKibben actuator with the controller matching the sensor output to a target value.

we expect SCP emulsions to unlock the sensorization of soft systems and facilitate the state feedback for a wide range of applications, including health monitoring, exploration, and robotic manipulation.

DISCUSSION

We have developed SCP emulsions that spontaneously form conductive composites upon printing. Our SCP emulsion used EtOH as a carrier solvent, rather than the conventional solvents, rendering a safe manufacturing process for conductive composites that are compatible with nearly any host substrate. We printed SCP emulsions onto numerous types of polymeric substrates, including sheets and textiles, to directly integrate sensing functionalities into soft-bodied systems. The printed sensors leveraged the opening of generic cracks that granted high sensitivity to strains and negligible hysteresis.

Printing strain sensors directly onto inflatable actuators demonstrated the viability of using SCP emulsions for the integration of sensors in all-soft systems. The EtOH medium of the SCP emulsion enabled printing of the conductive composite directly onto pressurized all-soft systems, a process that would otherwise lead to substrate damage due to the presence of conventional solvents in typical printable conductive composites. Such direct integration of sensors into soft systems unlocks opportunities to realize original soft actuators for which motion can be monitored in a seamless fashion. Our self-sensing McKibben actuator, which exploits a composite-infused balloon as its bladder, demonstrates the practical impact of SCP emulsions and their applications in robotics. By using the sensor data, the motion of the self-sensing McKibben actuator was effectively controlled in a closed loop with a state estimation error <3.0%.

We further demonstrated the capabilities of SCP emulsions by printing the conductive composite into textile substrates and realized wearable textile sensors. These textile sensors exhibited pristine fiber architecture as the emulsion conformally coated the fiber rovings, enabling stretchability and breathability. The gauge factor of these textile sensors varied from 7 to 150, and their working strain (linear region) ranged from 4 to 28%, depending on the fiber architecture of substrate textiles. Most of all, SCP emulsions enabled the safe and rapid manufacturability of state-of-the-art composite sensors (fig. S11).

We hypothesize that the electrical conductivity of the produced composites would be simple to modulate by substituting nanoparticles with alternate conductive fillers (e.g., carbon nanotubes and silver nanowires) in SCP emulsions (*47*, *48*). Increasing electrical conductivity of the produced composite will expand the potential application of SCP emulsions, such as stretchable electronics or textile electronics. In addition, material selections and processing parameters can be further investigated to enhance the quality of stand-alone composites and textile sensors. Chemistry and viscosity of the precursor, solvent liberation rate, and texture of the substrate are of interest. In the end, we anticipate the presented materials and fabrication strategies herein to

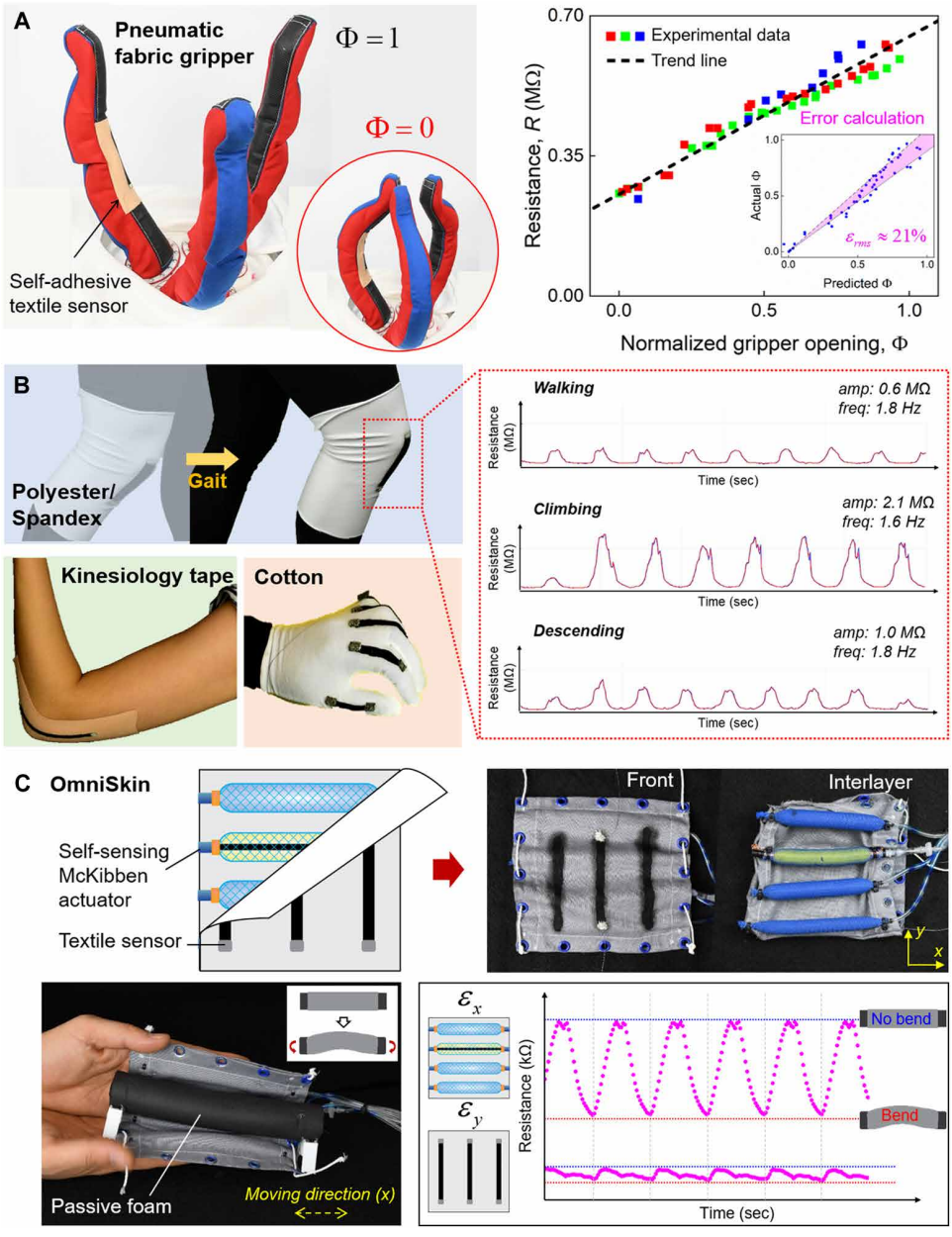

Fig. 7. Application of composite-infused textile sensors. (**A**) Composite-infused kinesiology tape attached to a pneumatic fabric gripper to monitor the grip opening ratio (Φ). This self-adhesive textile sensor can conform to the surface contours and measure the curvature upon gripping motion. (**B**) Active clothes that are easy to don/doff and elucidate a specific motion artifact present in normal human activities. Ready-made garments are also transformed into strain-sensing wearables (see fig. S10 for details). (**C**) OmniSkin, a hybrid of sensorized soft systems where composite sensors are printed onto bare polymer substrates and textiles, respectively. This robotic textile can monitor bidirectional strains applied to a passive foam during its inchworm motion via integrated self-sensing McKibben actuator (ε_x) and textile sensor (ε_y).

open a new avenue for forthcoming technologies beyond wearables and robotics.

MATERIALS AND METHODS

Materials

Room temperature vulcanizing amine cure silicone (SEMICOSIL 964 UV/CLEAR) was obtained from Wacker (Adrian, MI), and CB (BLACK PEARLS 2000) was purchased from Cabot (Boston, MA). Silver conductive epoxy (part no. 8331-14G) was obtained from MG Chemicals (Surrey, British Columbia), and a two-part silicone elastomer Ecoflex 00-30 was purchased from Smooth-On (Macungie, PA). Conductive Velcro (part no. 1324) and conductive thread (part no. 641) were purchased from Adafruit (New York City, NY). Polyester Lycra/Spandex four-way stretch fabric (LY 902) was obtained from Paylessfabric (Iva, SC) and used as is. Kinesiology tape (Tex Gold FP) and cotton gloves (Hycome white gloves) were purchased from Amazon (Seattle, WA).

Preparation and printing of SCP emulsions

A mixture of CB (0 to 1 g) and EtOH (100 ml) was prepared and sonicated using a tip sonicator Q700 from QSonica. Sonication pulse (1-s on/1-s off) was applied at 70% for 3 min to break up CB aggregates. PDMS resin (4 g) was then added to the CB/EtOH mixture, and an identical sonication pulse was applied for 1 min to emulsify the resin. Upon the completion of the process, the emulsion was moved onto 50-ml falcon tubes for characterization and/or sensor fabrication.

Direct printing was performed using a custom-made direct printing setup. The direct printing setup consists of a commercial three-dimensional printing machine (Simple Metal, PrintrBot) of which its filament feeder is substituted with a syringe pump. Substrate was placed on the stage of the setup, allowing the planar movement while the syringe pump enabled the feeding at 3.5 ml/min to write traces onto the substrate. Screen printing was performed by covering a substrate with an impermeable polyethylene terephthalate film where a specific shape was laser-cut. For the case of prestretched bare polymer substrates, a sheet of Ecoflex 00-30 was stretched 100% and fixed using adhesive tape, after which the screen-printing procedure was performed. A polycarbonate blade was moved across the film once the Pickering emulsion was poured to fill the open space of the film. The resulting substrates were dried at room conditions, and infused composites were cured subsequently. Prepared composite-coated substrates were tested after at least 1 hour from fabrication to ensure the complete cross-linking of the PDMS matrix.

Among the stretchable polymer substrates that we used (Ecoflex 00-30, Dragon Skin 10, and latex), no significant disparity was

detected in the resulting composite morphology. In detail, although an SCP emulsion wet latex (marginal polarity) better than silicone elastomers (negligible polarity), the relaxation of the colloids persisted in a similar fashion across the substrates. We thus speculate that the compatible wettability window for the SCP emulsion is large because it is the medium of the SCP emulsion that determines the wettability (EtOH in this study), which works as a vehicle for the active materials (CB/PDMS-precursor droplets).

Characterization of SCP emulsions

Dynamic light scattering was performed using a NanoBrook Omni from Brookhaven Instruments. The emulsion was diluted by 100:1 in EtOH and tested using the emission light of 350 nm and backscatter mode. At least five measurements were performed for each case, and error bars denote 1 SD. UV-vis measurement was performed using a Cary 100 from Varian. The emulsion was diluted in EtOH by 200:1 in volume and measured in a crystal cuvette for 120 min. Absorbance at a wavelength of 450 nm was used to quantify the settlement using absorbance retention $A_t/A_{t=0}$, where A_t denotes the measurement after t min. Rheometer tests were performed using an ARES LS1 from TA Instruments with parallel plates with a diameter of 15 mm at the oscillatory strain of 1.0%. A solvent trap was used to prevent the evaporation of EtOH during the measurement and test. SEM was performed using SU-70 from Hitachi. To image emulsified PDMS droplets, we added a light amount of deionized water to the emulsion and stirred for 30 min to promote curing of PDMS droplets within the emulsion. Freeze-fractured specimens were prepared by casting this cured droplet to epoxy and fracturing it after freezing using liquid nitrogen.

Characterization of the composites and sensors

The sheet resistance of composites, either printed onto bare polymer substrates or textiles, was measured by four-point measurements using a digital multimeter (model 34401A) from Agilent. The probe for the measurement was prepared with a 1-mm tip spacing, and liquid metal (eutectic gallium-indium alloy) was used to provide a low contact resistance. At least five measurements were performed for each case. SEM was used to reveal the composite surface morphology and the cross-sectional surface, and energy-dispersive x-ray spectroscopy (EDS) was performed at 10.0 kV within the SEM. TEM was performed using a Tecnai Osiris from FEI operated at 200 kV, and specimens were sectioned using a Leica EM UC7 cryo-microtome. Optical imaging was performed to analyze strain-responsive crack opening behavior of the composites using a Smartzoom 5 from Zeiss. The porosity of textile sensors were calculated using a conventional digital single-lens reflex camera with a backlight applied to the textile. The trace of EtOH after printing onto the textile was visualized by the slight addition of rhodamine dye to the EtOH before the sonication.

To obtain sensor characteristics of composite-printed specimens, we performed uniaxial cyclic tests using a dynamic testing machine E300 from Instron with the frequency at 7 Hz and displacement of 10 mm for specimens with a 60-mm gauge length. A specimen was cut to the dimension of $l = 75$ mm and $w = 5$ mm, and a copper tape was attached to both ends of the composite and encapsulated using duct tape to avoid electrical contact with the grips when loaded into the frame. Once a specimen was loaded, the copper tapes were connected to a custom-made Wheatstone bridge board consisting of three resistors (i.e., 100 kilohm and 8.2 megohm for bare polymer substrate and textile substrate, respectively) and a voltage follower to maintain the consistent input voltage throughout the test. The measured voltage from this board was directly sent to the software Bluehill (Instron) that simultaneously records stress-strain data.

Crack opening sensing mechanism

The crack opening ratio was defined as $\xi(\varepsilon) = l(\varepsilon)/l_{max}$, where $l(\varepsilon)$ is the length of a crack at strain ε and l_{max} is the length of a fully opened crack. Assuming that crack asperities are uniformly populated along the crack length (x direction) and each crack asperity provides constant electrical conductance when a pair of crack asperities are in contact, the local conductance S across a crack was predicted as

$$S = \int_0^{l_{max}-l} G_a \mu dx \; (l_0 \leq l \leq l_{max}) \quad (1)$$

where G_a is the conductance from a pair of connected crack asperities, μ is the density of crack asperities along the crack length, and l_0 is the initial length of crack (see fig. S2). This crack opening–driven mechanism was a modification of the crack asperity–driven mechanism in (*23*) and can be normalized by S_{max} (at l =0) to simplify as

$$\bar{S} = 1 - \xi \; (\xi_0 \leq \xi \leq 1) \quad (2)$$

where ξ_0 is determined from the initial crack length l_0.

Demonstration of soft systems with directly printed sensors

SCP emulsions were printed onto all-soft systems in their inflated state to complement stretchability of the produced composites (*49*). Commercial latex balloons were pressurized, and SCP emulsion was printed onto the surface, thereby creating conductive composites. For twisting latex balloons, a conductive copper tape enclosed both ends of the composite to provide electrical connection via conductive threads. Thus, electrical resistance of the composite was in situ monitored as the balloon inflated/deflated. For spherical latex balloons, their pressure and pertinent electrical resistance were intermittently measured as the balloon deflated. The pressure of the balloon was measured through a pressure sensor (part no. 5 INCH-G-4V, Amphenol) communicating with an Arduino, and the resistance of the sensor was manually measured using a multimeter.

Soft systems consisting of a silicone elastomer matrix (Ecoflex 00-30, Smooth-On) were prepared in a similar fashion with the latex balloons. A four-legged gripper was fabricated by casting the resin in a mold for a pneumatic chamber and adhering a strain-limiting muslin fabric (product no. 8808K11, McMaster-Carr) on the bottom of the chamber. The fiber-reinforced actuator and a strain-limiting layer were prepared as described in (*45*). SCP emulsions were printed onto these actuators after inflating them, and then, the pressurized air was removed to provide electrical connection after 30 min using a conductive carbon grease (part no. 8481-1, MG Chemicals). The electrical resistance of composites was in situ measured using a multimeter.

Self-sensing McKibben actuators were prepared by assembling a composite-printed twisting latex balloon and a strain-limiting mesh (PTN0.25BL, Techflex). Copper tapes enclosed both ends of the composite to provide robust electrical connection for alligator clips. The composite sensor was connected to a voltage divider to enable feedback control of the actuator. Ground truth sensor data were obtained by taking a series of photographs while maintaining a constant pressure in the unloaded actuator and measuring the

resistance across the sensor. The correlation between pressure and actuator length was nearly perfect (<1%) and was used for subsequent characterizations of the sensor response (under the same conditions) to build up a statistically viable sensor-to-length correlation. For closed-loop control of the actuators, an independent processor board (Arduino UNO) used the voltage divider to measure the resistance of the sensor, compared it to the target resistance value, and then sent appropriate command signals (in the form of a target pressure via a proportional gain multiplier) to an in-house–designed pressure regulator/sensor board.

Demonstration of composite-infused textiles sensors

Composite-infused kinesiology tape was fabricated by direct-printing an SCP emulsion onto the purchased kinesiology tapes. Conductive threads were then stitched to each end of the sensory trace using a conductive epoxy adhesive and used for the electrical connection. The same was applied to composite-infused kneepads and cotton gloves. The electrical resistance of the composite trace was measured using a custom-made Wheatstone bridge board attached to an Arduino.

Robotic skins (OmniSkins) were prepared by first printing an SCP emulsion onto muslin fabric. Then, we attached a self-sensing McKibben actuator and three conventional McKibben actuators onto the fabric. This robotic skin was wrapped around a passive polyethylene foam, and pneumatic pressure (~100 kPa) was applied to the actuators. Electrical resistance of the self-sensing actuator and textile sensor was monitored using a Wheatstone bridge and an Arduino microcontroller.

SUPPLEMENTARY MATERIALS

robotics.sciencemag.org/cgi/content/full/5/39/eaay3604/DC1
Fig. S1. Rheological profile of the SCP emulsion at different EtOH concentrations.
Fig. S2. Crack opening mechanism for strain sensing.
Fig. S3. Optical images of composite-infused polyester/spandex textile.
Fig. S4. Separation of EtOH from CB/PDMS-precursor droplets on a textile.
Fig. S5. Cross-sectional SEM image of SCP emulsion–printed textile.
Fig. S6. Tensile moduli of composite-infused textiles.
Fig. S7. Fatigue resistance of composite-infused polyester/spandex textiles.
Fig. S8. Shape estimation of an inflatable latex balloon.
Fig. S9. Fabric gripper with a stand-alone sensor and a self-adhesive sensor.
Fig. S10. Strain sensing of composite-infused textiles fabricated from ready-made garments.
Fig. S11. Comparison with existing manufacturing processes for composite sensors.
Movie S1. Direct comparison of SCP emulsion (EtOH) and conventional suspension (cyclohexane) on a latex balloon.
Movie S2. Sensorized latex balloon using an SCP emulsion.
Movie S3. Fiber-reinforced actuator with an SCP emulsion–printed trace and a self-adhesive strain-limiting layer.
Movie S4. Closed-loop control of a self-sensing McKibben actuator.
Movie S5. SCP emulsion–printed kinesiology tape to measure elbow flexion.
Movie S6. Hybrid robotic textile (OmniSkin) giving rise to an inchworm motion.
References (*50*–*70*)

REFERENCES AND NOTES

1. R.-H. Kim, D.-H. Kim, J. Xiao, B. H. Kim, S.-I. Park, B. Panilaitis, R. Ghaffari, J. Yao, M. Li, Z. Liu, V. Malyarchuk, D. G. Kim, A. P. le, R. G. Nuzzo, D. L. Kaplan, F. G. Omenetto, Y. Huang, Z. Kang, J. A. Rogers, Waterproof AlInGaP optoelectronics on stretchable substrates with applications in biomedicine and robotics. *Nat. Mater.* **9**, 929–937 (2010).
2. S.-K. Kang, R. K. J. Murphy, S.-W. Hwang, S. M. Lee, D. V. Harburg, N. A. Krueger, J. Shin, P. Gamble, H. Cheng, S. Yu, Z. Liu, J. G. McCall, M. Stephen, H. Ying, J. Kim, G. Park, R. C. Webb, C. H. Lee, S. Chung, D. S. Wie, A. D. Gujar, B. Vemulapalli, A. H. Kim, K.-M. Lee, J. Cheng, Y. Huang, S. H. Lee, P. V. Braun, W. Z. Ray, J. A. Rogers, Bioresorbable silicon electronic sensors for the brain. *Nature* **530**, 71–76 (2016).
3. J. Xu, S. Wang, G. J. N. Wang, C. Zhu, S. Luo, L. Jin, X. Gu, S. Chen, V. R. Feig, J. W. F. To, S. Rondeau-Gagné, J. Park, B. C. Schroeder, C. Lu, J. Y. Oh, Y. Wang, Y.-H. Kim, H. Yan, R. Sinclair, D. Zhou, G. Xue, B. Murmann, C. Linder, W. Cai, J. B.-H. Tok, J. W. Chung, Z. Bao, Highly stretchable polymer semiconductor films through the nanoconfinement effect. *Science* **355**, 59–64 (2017).
4. J. A. Rogers, T. Someya, Y. Huang, Materials and mechanics for stretchable electronics. *Science* **327**, 1603–1607 (2010).
5. M. Amjadi, K.-U. Kyung, I. Park, M. Sitti, Stretchable, skin-mountable, and wearable strain sensors and their potential applications: A review. *Adv. Funct. Mater.* **26**, 1678–1698 (2016).
6. B. T. Quinlivan, S. Lee, P. Malcolm, D. M. Rossi, M. Grimmer, C. Siviy, N. Karavas, D. Wagner, A. Asbeck, I. Galiana, C. J. Walsh, Assistance magnitude versus metabolic cost reductions for a tethered multiarticular soft exosuit. *Sci. Robot.* **2**, eaah4416 (2017).
7. Y. Wei, Q. Xu, An overview of micro-force sensing techniques. *Sens. Actuators A Phys.* **234**, 359–374 (2015).
8. M. Xie, K. Hisano, M. Zhu, T. Toyoshi, M. Pan, S. Okada, O. Tsutsumi, S. Kawamura, C. Bowen, Flexible multifunctional sensors for wearable and robotic applications. *Adv. Mater. Dent. Tech.* **4**, 1800626 (2019).
9. D. Rus, M. T. Tolley, Design, fabrication and control of soft robots. *Nature* **521**, 467–475 (2015).
10. C. Laschi, B. Mazzolai, M. Cianchetti, Soft robotics: Technologies and systems pushing the boundaries of robot abilities. *Sci. Robot.* **1**, eaah3690 (2016).
11. M. A. Robertson, H. Sadeghi, J. M. Florez, J. Paik, Soft pneumatic actuator fascicles for high force and reliability. *Soft Robot.* **4**, 23–32 (2017).
12. T. J. Wallin, J. Pikul, R. F. Shepherd, 3D printing of soft robotic systems. *Nat. Rev. Mater.* **3**, 84–100 (2018).
13. S. Lee, A. Reuveny, J. Reeder, S. Lee, H. Jin, Q. Liu, T. Yokota, T. Sekitani, T. Isoyama, Y. Abe, Z. Suo, T. Someya, A transparent bending-insensitive pressure sensor. *Nat. Nanotechnol.* **11**, 472–478 (2016).
14. N. Matsuhisa, D. Inoue, P. Zalar, H. Jin, Y. Matsuba, A. Itoh, T. Yokota, D. Hashizume, T. Someya, Printable elastic conductors by in situ formation of silver nanoparticles from silver flakes. *Nat. Mater.* **16**, 834–840 (2017).
15. D. J. Lipomi, M. Vosgueritchian, B. C. K. Tee, S. L. Hellstrom, J. A. Lee, C. H. Fox, Z. Bao, Skin-like pressure and strain sensors based on transparent elastic films of carbon nanotubes. *Nat. Nanotechnol.* **6**, 788–792 (2011).
16. W. Hu, X. Niu, R. Zhao, Q. Pei, Elastomeric transparent capacitive sensors based on an interpenetrating composite of silver nanowires and polyurethane. *Appl. Phys. Lett.* **102**, 083303 (2013).
17. A. Atalay, V. Sanchez, O. Atalay, D. M. Vogt, F. Haufe, R. J. Wood, C. J. Walsh, Batch fabrication of customizable silicone-textile composite capacitive strain sensors for human motion tracking. *Adv. Mater. Technol.* **2**, 1700136 (2017).
18. K. Li, H. Wei, W. Liu, H. Meng, P. Zhang, C. Yan, 3D printed stretchable capacitive sensors for highly sensitive tactile and electrochemical sensing. *Nanotechnology* **29**, 185501 (2018).
19. K. R. Phillips, G. T. England, S. Sunny, E. Shirman, T. Shirman, N. Vogel, J. Aizenberg, A colloidoscope of colloid-based porous materials and their uses. *Chem. Soc. Rev.* **45**, 281–322 (2016).
20. T. G. Thuruthel, B. Shih, C. Laschi, M. T. Tolley, Soft robot perception using embedded soft sensors and recurrent neural networks. *Sci. Robot.* **4**, eaav1488 (2019).
21. C. Pang, G.-Y. Lee, T.-i. Kim, S. M. Kim, H. N. Kim, S.-H. Ahn, K. Y. Suh, A flexible and highly sensitive strain-gauge sensor using reversible interlocking of nanofibres. *Nat. Mater.* **11**, 795–801 (2012).
22. J. Kim, M. Lee, H. J. Shim, R. Ghaffari, H. R. Cho, D. Son, Y. H. Jung, M. Soh, C. Choi, S. Jung, K. Chu, D. Jeon, S.-T. Lee, J. H. Kim, S. H. Choi, T. Hyeon, D. H. Kim, Stretchable silicon nanoribbon electronics for skin prosthesis. *Nat. Commun.* **5**, 5747 (2014).
23. D. Kang, P. V. Pikhitsa, Y. W. Choi, C. Lee, S. S. Shin, L. Piao, B. Park, K.-Y. Suh, T.-i. Kim, M. Choi, Ultrasensitive mechanical crack-based sensor inspired by the spider sensory system. *Nature* **516**, 222–226 (2014).
24. B. Xu, A. Akhtar, Y. Liu, H. Chen, W.-H. Yeo, S. I. Park, B. Boyce, H. Kim, J. Yu, H. Y. Lai, S. Jung, Y. Zhou, J. Kim, S. Cho, Y. Huang, T. Bretl, J. A. Rogers, An epidermal stimulation and sensing platform for sensorimotor prosthetic control, management of lower back exertion, and electrical muscle activation. *Adv. Mater.* **28**, 4462–4471 (2016).
25. C. Majidi, R. Kramer, R. J. Wood, A non-differential elastomer curvature sensor for softer-than-skin electronics. *Smart Mater. Struct.* **20**, 105017 (2011).
26. J. T. Muth, D. M. Vogt, R. L. Truby, Y. Mengüç, D. B. Kolesky, R. J. Wood, J. A. Lewis, Embedded 3d printing of strain sensors within highly stretchable elastomers. *Adv. Mater.* **26**, 6307–6312 (2014).
27. J.-Y. Sun, C. Keplinger, G. M. Whitesides, Z. Suo, Ionic skin. *Adv. Mater.* **26**, 7608–7614 (2014).
28. C. Larson, B. Peele, S. Li, S. Robinson, M. Totaro, L. Beccai, B. Mazzolai, R. Shepherd, Highly stretchable electroluminescent skin for optical signaling and tactile sensing. *Science* **351**, 1071–1074 (2016).
29. F. Hussain, M. Hojjati, M. Okamoto, R. E. Gorga, Review article: Polymer-matrix nanocomposites, processing, manufacturing, and application: An overview. *J. Compos. Mater.* **40**, 1511–1575 (2006).

30. E. L. White, M. C. Yuen, J. C. Case, R. K. Kramer, Low-cost, facile, and scalable manufacturing of capacitive sensors for soft systems. *Adv. Mater. Technol.* **2**, 1700072 (2017).
31. S. Y. Kim, T.-W. Lim, N. R. Sottos, S. R. White, Manufacture of carbon-fiber prepreg with thermoplastic/epoxy resin blends and microencapsulated solvent healing agents. *Compos. Part A Appl. Sci. Manuf.* **121**, 365–375 (2019).
32. M. S. Easmin, M. Z. I. Sarker, S. Ferdosh, S. H. Shamsudin, K. B. Yunus, M. S. Uddin, M. M. R. Sarker, M. J. H. Akanda, M. S. Hossain, H. P. S. A. Khalil, Bioactive compounds and advanced processing technology: *Phaleria macrocarpa* (sheff.) Boerl, a review. *J. Chem. Technol. Biotechnol.* **90**, 981–991 (2015).
33. E. Browning, *Toxicity of Industrial Organic Solvents* (Chemical Pub. Co., 1953); http://agris.fao.org/agris-search/search.do?recordID=US201300637470.
34. J. N. Lee, C. Park, G. M. Whitesides, Solvent compatibility of poly(dimethylsiloxane)-based microfluidic devices. *Anal. Chem.* **75**, 6544–6554 (2003).
35. S. U. Pickering, CXCVI.—Emulsions. *J. Chem. Soc. Trans.* **91**, 2001–2021 (1907).
36. A. Gelot, W. Friesen, H. A. Hamza, Emulsification of oil and water in the presence of finely divided solids and surface-active agents. *Colloids Surf.* **12**, 271–303 (1984).
37. R. M. Choueiri, E. Galati, H. Thérien-Aubin, A. Klinkova, E. M. Larin, A. Querejeta-Fernández, L. Han, H. L. Xin, O. Gang, E. B. Zhulina, M. Rubinstein, E. Kumacheva, Surface patterning of nanoparticles with polymer patches. *Nature* **538**, 79–83 (2016).
38. B. Furie, B. C. Furie, The molecular basis of blood coagulation. *Cell* **53**, 505–518 (1988).
39. A. J. Singer, R. A. F. Clark, Cutaneous wound healing. *N. Engl. J. Med.* **341**, 738–746 (1999).
40. S. Iijima, P. M. Ajayan, Substrate and size effects on the coalescence of small particles. *J. Appl. Phys.* **70**, 5138–5140 (1991).
41. B. Michen, C. Geers, D. Vanhecke, C. Endes, B. Rothen-Rutishauser, S. Balog, A. Petri-Fink, Avoiding drying-artifacts in transmission electron microscopy: Characterizing the size and colloidal state of nanoparticles. *Sci. Rep.* **5**, 9793 (2015).
42. S. Y. Kim, A. R. Jones, N. R. Sottos, S. R. White, Manufacturing of unidirectional glass/epoxy prepreg with microencapsulated liquid healing agents. *Compos. Sci. Technol.* **153**, 190–197 (2017).
43. J. Diani, B. Fayolle, P. Gilormini, A review on the Mullins effect. *Eur. Polym. J.* **45**, 601–612 (2009).
44. F. Ilievski, A. D. Mazzeo, R. F. Shepherd, X. Chen, G. M. Whitesides, Soft robotics for chemists. *Angew. Chem.* **123**, 1930–1935 (2011).
45. S. Y. Kim, R. Baines, J. Booth, N. Vasios, K. Bertoldi, R. Kramer-Bottiglio, Reconfigurable soft body trajectories using unidirectionally stretchable composite laminae. *Nat. Commun.* **10**, 3464 (2019).
46. J. W. Booth, D. Shah, J. C. Case, E. L. White, M. C. Yuen, O. Cyr-Choiniere, R. Kramer-Bottiglio, OmniSkins: Robotic skins that turn inanimate objects into multifunctional robots. *Sci. Robot.* **3**, eaat1853 (2018).
47. A. Kamyshny, M. Ben-Moshe, S. Aviezer, S. Magdassi, Ink-jet printing of metallic nanoparticles and microemulsions. *Macromol. Rapid Commun.* **26**, 281–288 (2005).
48. Y. Kim, J. Zhu, B. Yeom, M. di Prima, X. Su, J.-G. Kim, S. J. Yoo, C. Uher, N. A. Kotov, Stretchable nanoparticle conductors with self-organized conductive pathways. *Nature* **500**, 59–63 (2013).
49. D.-Y. Khang, J. A. Rogers, H. H. Lee, Mechanical buckling: Mechanics, metrology, and stretchable electronics. *Adv. Funct. Mater.* **19**, 1526–1536 (2009).
50. S. Yao, Y. Zhu, Wearable multifunctional sensors using printed stretchable conductors made of silver nanowires. *Nanoscale* **6**, 2345–2352 (2014).
51. A. Frutiger, J. T. Muth, D. M. Vogt, Y. Mengüç, A. Campo, A. D. Valentine, C. J. Walsh, J. A. Lewis, Capacitive soft strain sensors via multicore-shell fiber printing. *Adv. Mater.* **27**, 2440–2446 (2015).
52. E. Roh, B.-U. Hwang, D. Kim, B.-Y. Kim, N.-E. Lee, Stretchable, transparent, ultrasensitive, and patchable strain sensor for human-machine interfaces comprising a nanohybrid of carbon nanotubes and conductive elastomers. *ACS Nano* **9**, 6252–6261 (2015).
53. J. Shintake, E. Piskarev, S. H. Jeong, D. Floreano, Ultrastretchable strain sensors using carbon black-filled elastomer composites and comparison of capacitive versus resistive sensors. *Adv. Mater. Technol.* **3**, 1700284 (2018).
54. Y. Zhang, C. J. Sheehan, J. Zhai, G. Zou, H. Luo, J. Xiong, Y. T. Zhu, Q. X. Jia, Polymer-embedded carbon nanotube ribbons for stretchable conductors. *Adv. Mater.* **22**, 3027–3031 (2010).
55. D. J. Cohen, D. Mitra, K. Peterson, M. M. Maharbiz, A highly elastic, capacitive strain gauge based on percolating nanotube networks. *Nano Lett.* **12**, 1821–1825 (2012).
56. M. Amjadi, A. Pichitpajongkit, S. Lee, S. Ryu, I. Park, Highly stretchable and sensitive strain sensor based on silver nanowire–elastomer nanocomposite. *ACS Nano* **8**, 5154–5163 (2014).
57. N. Lu, C. Lu, S. Yang, J. Rogers, Highly sensitive skin-mountable strain gauges based entirely on elastomers. *Adv. Funct. Mater.* **22**, 4044–4050 (2012).
58. Y. R. Jeong, H. Park, S. W. Jin, S. Y. Hong, S. S. Lee, J. S. Ha, Highly stretchable and sensitive strain sensors using fragmentized graphene foam. *Adv. Funct. Mater.* **25**, 4228–4236 (2015).
59. T. Yamada, Y. Hayamizu, Y. Yamamoto, Y. Yomogida, A. Izadi-Najafabadi, D. N. Futaba, K. Hata, A stretchable carbon nanotube strain sensor for human-motion detection. *Nat. Nanotechnol.* **6**, 296–301 (2011).
60. L. Cai, L. Song, P. Luan, Q. Zhang, N. Zhang, Q. Gao, D. Zhao, X. Zhang, M. Tu, F. Yang, W. Zhou, Q. Fan, J. Luo, W. Zhou, P. M. Ajayan, S. Xie, Super-stretchable, transparent carbon nanotube-based capacitive strain sensors for human motion detection. *Sci. Rep.* **3**, 3048 (2013).
61. M. Amjadi, Y. J. Yoon, I. Park, Ultra-stretchable and skin-mountable strain sensors using carbon nanotubes-Ecoflex nanocomposites. *Nanotechnology* **26**, 375501 (2015).
62. B.-U. Hwang, J.-H. Lee, T. Q. Trung, E. Roh, D.-I. Kim, S.-W. Kim, N.-E. Lee, Transparent stretchable self-powered patchable sensor platform with ultrasensitive recognition of human activities. *ACS Nano* **9**, 8801–8810 (2015).
63. C. S. Boland, U. Khan, C. Backes, A. O'Neill, J. McCauley, S. Duane, R. Shanker, Y. Liu, I. Jurewicz, A. B. Dalton, J. N. Coleman, Sensitive, high-strain, high-rate bodily motion sensors based on graphene–rubber composites. *ACS Nano* **8**, 8819–8830 (2014).
64. X. Xiao, L. Yuan, J. Zhong, T. Ding, Y. Liu, Z. Cai, Y. Rong, H. Han, J. Zhou, Z. L. Wang, High-strain sensors based on ZnO nanowire/polystyrene hybridized flexible films. *Adv. Mater.* **23**, 5440–5444 (2011).
65. U.-H. Shin, D.-W. Jeong, S.-M. Park, S.-H. Kim, H.-W. Lee, J.-M. Kim, Highly stretchable conductors and piezocapacitive strain gauges based on simple contact-transfer patterning of carbon nanotube forests. *Carbon* **80**, 396–404 (2014).
66. J.-H. Kong, N. S. Jang, S. H. Kim, J. M. Kim, Simple and rapid micropatterning of conductive carbon composites and its application to elastic strain sensors. *Carbon* **77**, 199–207 (2014).
67. S. Gong, D. T. H. Lai, Y. Wang, L. W. Yap, K. J. Si, Q. Shi, N. N. Jason, T. Sridhar, H. Uddin, W. Cheng, Tattoolike polyaniline microparticle-doped gold nanowire patches as highly durable wearable sensors. *ACS Appl. Mater. Interfaces* **7**, 19700–19708 (2015).
68. S. Gong, D. T. H. Lai, B. Su, K. J. Si, Z. Ma, L. W. Yap, P. Guo, W. Cheng, Highly stretchy black gold E-skin nanopatches as highly sensitive wearable biomedical sensors. *Adv. Electron. Mater.* **1**, 1400063 (2015).
69. Y. Zheng, Y. Li, K. Dai, Y. Wang, G. Zheng, C. Liu, C. Shen, A highly stretchable and stable strain sensor based on hybrid carbon nanofillers/polydimethylsiloxane conductive composites for large human motions monitoring. *Compos. Sci. Technol.* **156**, 276–286 (2018).
70. Y. Wang, J. Balowski, C. Phillips, R. Phillips, C. E. Sims, N. L. Allbritton, Benchtop micromolding of polystyrene by soft lithography. *Lab Chip* **11**, 3089–3097 (2011).

Acknowledgments: We thank J. Jacobs for assisting with demonstrations of the sensor and E. Brown and A. M. Dollar for access to testing equipment. The pneumatic fabric gripper was provided by Otherlab for demonstration. **Funding:** This work was supported by a Small Business Technology Transfer (80NSSC17C0030) from NASA and a Faculty Early Career Development Award (CMMI-1454284) from NSF. C.O.O. and Y.C. acknowledge NSF support (DMR-1410568). R.A.B. acknowledges NSF support (EFRI-1830870). D.S.S. acknowledges NASA support (Space Technology Research Fellowship, 80NSSC17K0164). **Author contributions:** S.Y.K. and R.K.-B. conceived the idea. S.Y.K., Y.C., and G.K. performed the material characterization. S.Y.K., R.A.B., M.C.Y., and D.S.S. performed manufacturing and demonstration. C.O.O. and R.K.-B. reviewed and commented on the manuscript. All authors participated in writing the manuscript. **Competing interests:** The authors declare that they have no competing interests. **Data and materials availability:** All data are available in the main text or the Supplementary Materials.

Submitted 12 June 2019
Resubmitted 9 January 2020
Accepted 6 February 2020
Published 26 February 2020
10.1126/scirobotics.aay3604

Citation: S. Y. Kim, Y. Choo, R. A. Bilodeau, M. C. Yuen, G. Kaufman, D. S. Shah, C. O. Osuji, R. Kramer-Bottiglio, Sustainable manufacturing of sensors onto soft systems using self-coagulating conductive Pickering emulsions. *Sci. Robot.* **5**, eaay3604 (2020).

Science Robotics

Sustainable manufacturing of sensors onto soft systems using self-coagulating conductive Pickering emulsions

Sang Yup Kim, Youngwoo Choo, R. Adam Bilodeau, Michelle C. Yuen, Gilad Kaufman, Dylan S. Shah, Chinedum O. Osuji, and Rebecca Kramer-Bottiglio

Sci. Robot. **5** (39), eaay3604. DOI: 10.1126/scirobotics.aay3604

Science Robotics (ISSN 2470-9476) is published by the American Association for the Advancement of Science. 1200 New York Avenue NW, Washington, DC 20005. The title *Science Robotics* is a registered trademark of AAAS.